Original Article

JCBFM

Journal of Cerebral Blood Flow & Metabolism
2018, Vol. 38(1) 58–74

DOI: 10.1177/0271678X17705973
journals.sagepub.com/home/jcbfm
SAGE

mTOR drives cerebral blood flow and memory deficits in LDLR$^{-/-}$ mice modeling atherosclerosis and vascular cognitive impairment

Jordan B Jahrling[1], Ai-Ling Lin[2], Nicholas DeRosa[1], Stacy A Hussong[1], Candice E Van Skike[1], Milena Girotti[3], Martin Javors[4], Qingwei Zhao[5], Leigh Ann Maslin[6], Reto Asmis[6,7] and Veronica Galvan[1]

Abstract

We recently showed that mTOR attenuation blocks progression and abrogates established cognitive deficits in Alzheimer's disease (AD) mouse models. These outcomes were associated with the restoration of cerebral blood flow (CBF) and brain vascular density (BVD) resulting from relief of mTOR inhibition of NO release. Recent reports suggested a role of mTOR in atherosclerosis. Because mTOR drives aging and vascular dysfunction is a universal feature of aging, we hypothesized that mTOR may contribute to brain vascular and cognitive dysfunction associated with atherosclerosis. We measured CBF, BVD, cognitive function, markers of inflammation, and parameters of cardiovascular disease in LDLR$^{-/-}$ mice fed maintenance or high-fat diet ± rapamycin. Cardiovascular pathologies were proportional to severity of brain vascular dysfunction. Aortic atheromas were reduced, CBF and BVD were restored, and cognitive dysfunction was attenuated potentially through reduction in systemic and brain inflammation following chronic mTOR attenuation. Our studies suggest that mTOR regulates vascular integrity and function and that mTOR attenuation may restore neurovascular function and cardiovascular health. Together with our previous studies in AD models, our data suggest mTOR-driven vascular damage may be a mechanism shared by age-associated neurological diseases. Therefore, mTOR attenuation may have promise for treatment of cognitive impairment in atherosclerosis.

Keywords

Atherosclerosis, cerebral blood flow, cognition, inflammation, vascular biology

Received 8 July 2016; Revised 1 February 2017; Accepted 27 February 2017

Introduction

The symptomatic pathology of neurodegeneration such as that associated with Alzheimer's disease (AD) results from prolonged dysfunction at a cellular level that precedes symptoms by years and likely even decades.[1] It is well established that many of the known risk factors for

[1]Department of Cellular and Integrative Physiology and The Barshop Institute for Longevity and Aging Studies, University of Texas Health Science Center at San Antonio, TX, USA
[2]Sanders-Brown Center on Aging, Department of Pharmacology and Nutritional Sciences and Department of Biomedical Engineering, University of Kentucky, KY, USA
[3]Department of Pharmacology, University of Texas Health Science Center at San Antonio, TX, USA
[4]Department of Psychiatry, University of Texas Health Science Center at San Antonio, TX, USA
[5]Department of Medicine, University of Texas Health Science Center at San Antonio, TX, USA
[6]Department of Clinical Laboratory Sciences, University of Texas Health Science Center at San Antonio, TX, USA
[7]Department of Biochemistry, University of Texas Health Science Center at San Antonio, TX, USA

Corresponding author:
Veronica Galvan, University of Texas Health Science Center at San Antonio, 15355 Lambda Drive, San Antonio, TX 78212, USA.
Email: galvanv@uthscsa.edu

AD and other dementias prominently include cardiovascular dysfunction and atherosclerosis.[2,3] These disease processes have profound effects on both peripheral and central vascular function,[4,5] and thus improvement of cardiovascular capacity also enhances cognitive function in humans.[6–8] Accordingly, in an effort to develop early stage interventions, the investigation of known risk factor mechanisms and contributions to AD pathogenesis are active areas of research.

Serum cholesterol levels prominently factor in the development of cardiovascular disease[9] and abnormal cholesterol metabolism is increasingly being linked with cognitive impairment.[10,11] Members of the lipoprotein family are tasked with the transport of cholesterol, triglycerides, and phospholipids. Increasing blood levels of the low density lipoprotein (LDL) have been associated with atherosclerosis and cardiovascular disease,[12] which are themselves recognized as risk factors for dementias.[2,3,13] In humans, gene mutations of the LDL receptor (LDLR), which removes LDL from the circulation via endocytosis, result in familial hypercholesterolemia,[14] a condition that is linked to premature coronary heart disease.[15] LDLR also recognizes apolipoprotein E (ApoE) which is believed to play a significant role in AD pathogenesis.[3]

The LDLR knock out mouse ($LDLR^{-/-}$) is a model for atherosclerosis and related cardiac dysfunction. These mice exhibit significant elevations in plasma cholesterol and rapid, progressive development of atherosclerosis, further exacerbated by a high fat diet (HFD). While cognitive deficits in $LDLR^{-/-}$ mice were suggested,[16,17] little is known regarding the extent or mechanisms of dysfunction and their relation with hypercholesterolemia and brain vascular damage. In the present study, we measured parameters of peripheral and central vascular function, determined cognitive outcomes as specific forms of learning and memory, and defined the role of mTOR in maintenance- or HFD-fed $LDLR^{-/-}$ mice. As suggested by previous studies,[18,19] systemic attenuation of mTOR with rapamycin reduced atherosclerotic lesions. In addition, we report that mTOR attenuation abolished profound functional and structural neurovascular deficits and ameliorated memory impairment in $LDLR^{-/-}$ animals, while reducing parameters of vascular and systemic inflammation. Our studies suggest a critical role of mTOR in mechanisms of neurovascular damage associated with inflammatory processes of atherosclerosis. Attenuating mTOR activity, an intervention that extends lifespan and improves critical aspects of healthspan in mice, including the restoration of cognitive function in mouse models of AD, may also be of value in the treatment of cognitive impairment associated with atherosclerosis.

Materials and methods

Animal, diets and experimental design

All studies were performed under approval of the UTHSCSA Institutional Animal Care and Use Committee (Animal Welfare Assurance Number: A3345-01) – which adheres to the Animal Welfare Act, the *Guide for the Care and Use of Laboratory Animals*, the Public Health Service Policy on Humane Care and Use of Laboratory Animals, and the US Government Principles for the Utilization and Care of Vertebrate Animals Used in Testing, Research, and Training – and also in compliance with the ARRIVE guidelines (Animal Research: Reporting In Vivo Experiments) for reporting animal experiments. Group size calculations for in vivo experiments were based on MWM because it has the highest variability. We estimated group sizes of $n = 12$ as sufficient to provide .85 power to detect an effect $f = 0.4$ with overall $SD = 15\%$ and $alpha = 0.05$ in RM-ANOVA). SAA and IL-6 were measured in serum and brain of the same animals that were tested in the MWM, respectively. CBF studies utilized animals that were not included in MWM and had been generated to be matched for age with those in MWM studies. From our prior studies,[20] we determined that five mice per group would provide .8 power to detect an effect $f = 0.9$ with overall $SD = 7\%$ and $alpha = 0.05$ in ANOVA. We verified that our MWM and CBF studies were adequately powered ($n = 4$ to have .85 power to detect an effect $f = 1.15$ with overall $SD = 10.4\%$ and $alpha = 0.05$ in ANOVA, and $n = 9$ to have 0.84 power to detect an effect $f = 1.36$ with overall $SD = 9.5\%$ and $alpha = 0.05$ in RM-ANOVA for MWM and CBF studies respectively). Studies of brain vascular density (BVD) using $n = 4$ provided .85 power to detect an effect $f = 1.14$ with overall $SD = 6.33\%$ at $alpha = 0.5$ in ANOVA. HFD-fed $LDLR^{-/-}$ mice showed accelerated weight loss and high mortality as a result of intraperitoneal injection of rapamycin; thus, this group was removed from ANOVA of CBF and VD data.

Tissues from animals that were used in CBF experiments were not utilized for any other determinations. For all studies, treatment groups were randomized by parentage. We minimized potential misidentification of animals in behavioral and functional imaging studies by using unique animal identifiers that were permanently tattooed on the tail.

Aortic arch lesion area studies used estimated group sizes of $n = 6$ as sufficient to provide .95 power to detect an effect $f = 0.5$ with overall $SD = 5\%$ and $alpha = 0.05$ in 2W-ANOVA. For comparisons of two independent means group sizes using t tests, we estimated group sizes of $n = 6$ as sufficient to provide 0.8 power to detect an effect $d = 1.8$ with overall $SD = 5\%$ and

alpha = 0.05 in two-tailed Student's t test. For ventricle mass studies, we estimated group sizes of n = 8 as sufficient to provide 0.8 power to detect an effect $f = 0.38$ with overall SD = 8% and alpha = 0.05 in two-way ANOVA.

Personnel performing experiments identified animals only by the animal identifier and were blinded from genotype and treatment assignment. Male and female $LDLR^{-/-}$ (B6.129S7-$Ldlr^{tm1Her}$/J, Jackson Laboratories, Bar Harbor, ME) or C57Bl/6 (hereafter referred to as 'WT', Jackson Laboratories, Bar Harbor, ME) mice were housed ≤5/cage and maintained on a 12-h light/12-h dark cycle. WT and $LDLR^{-/-}$ mice were fed maintenance (AIN-76A, BioServ) diet, while additional $LDLR^{-/-}$ mice were fed high fat diet (HFD; 21% saturated milk fat, 0.2% cholesterol, supplemented into AIN-76A, BioServ). Encapsulated rapamycin (14 ppm) prepared as described[21] was supplemented into HFD. Control HF diet was also prepared which contained eudragit only (HF Eud); Eudragit is the encapsulation material for rapamycin that aids in enteric drug absorption. Animals were euthanized by isoflurane overdose followed by cervical dislocation or by CO_2 overdose followed by cervical dislocation. Brain was dissected within ~1.5–2 min of death. Blood was collected post-mortem from heart.

Animal cohorts

Cohort 1: mice of both sexes were treated at 8–10 weeks of age for 10, 20 or 30 weeks, corresponding to expected aortic lesion states I and II, I, II and III and I, II, III and IV. Cohort 2: males aged to 28 weeks were treated intraperitoneally (IP) with either rapamycin (10 mg/kg) or vehicle every other day for 16 weeks, at which time MRI studies to investigate CBF and BVD were performed. IP administration of rapamycin was utilized for these studies due to temporary unavailability of supplemented chow due to licensing of the formulation; IP delivery of rapamycin has been shown to be equivalent to enteric delivery via chow supplementation.[22] Cohort 3: a crossover design in which mice were fed a HFD +/− rapamycin for 15 weeks starting at 20 weeks of age, then switched to the opposite diet for 15 weeks. Cohort 4: an all-male group fed maintenance or HFD +/− rapamycin beginning at 28 weeks of age for 20 weeks. Only males were used to avoid potential confounds related to variability in female performance in the Morris water maze (MWM).[23,24] All behavioral testing was performed at 12 months of age. Prior studies reported cognitive deficits in $LDLR^{-/-}$ mice at seven to eight months of age[25]; since we aimed to model treatment and not prevention of these deficits, Cohort 2 and 4 studies were designed accordingly.

Note: The $LDLR^{-/-}$ model of atherosclerosis relies on the use of HFD. In an effort to remain consistent with prior knowledge in the field, we designed our experiments such that the efficacy of mTOR inhibition by rapamycin was tested in the best-established $LDLR^{-/-}$ model of atherosclerosis, using HFD-fed LDL mice treated with Eudragit-supplemented or rapamycin-supplemented chow. Due to time limitations, a maximum of 60 animals can be tested in the Morris water maze (MWM) in a single study. Accordingly, maintenance chow-fed $LDLR^{-/-}$, rapamycin-fed groups were excluded for all experiments with the exception of Cohort 2 (MRI-based studies, Figure 4). The inclusion of maintenance chow-fed $LDLR^{-/-}$ rapamycin-fed groups in MRI studies was possible in MRI studies because sample sizes adequate to identify differences in group means for those measures were smaller than those calculated for MWM studies.

Blood analysis

Mice were fasted overnight and sacrificed with blood collection via cardiac puncture. Rapamycin levels in whole blood were determined at 30 weeks by LC/MS. Remaining blood was centrifuged and plasma samples were collected and analyzed for total cholesterol (Total Cholesterol E Kit, Wako Chemicals, Richmond, VA) and trigylycerides (L-type Triglycerides M, Wako Chemicals, Richmond, VA).

Fasting glucose

Mice were fasted overnight for 16 h. Blood was collected from the tail vein and tested using a handheld glucose monitor (LifeScan One Touch Ultra).

Measurement of rapamycin (RAPA) using HPLC-tandem MS

The HPLC system consisted of a Shimadzu SCL-10A Controller, LC-10AD pump with a FCV-10AL mixing chamber, SIL-10AD autosampler, and an AB Sciex API 3200 tandem mass spectrometer with turbo ion spray. The analytical column was a Grace Alltima C18 (4.6 × 150 mm, 5 µ; Alltech (Deerfield, IL)) and was maintained at 60°C during the chromatographic runs in a Shimadzu CTO-10A column oven. Additional details are available in the supplementary materials.

Measurement of markers of inflammation

Serum amyloid A (SAA) was measured in serum using an SAA ELISA Kit (Invitrogen). Briefly, samples were diluted in diluent buffer and added to microplate wells in duplicate. An equivalent volume of anti-SAA HRP

was added and the plate was covered and incubated for 1 h at 37°C. Wells were then gently aspirated, washed 4× with wash buffer, and substrate was added to each well. The plate was covered and incubated for 15 min at RT. After addition of stop solution, absorbance at 450 nm was measured using 630 nm as a reference.

Total RNA extraction

RNA extracts were prepared from microvessel-depleted brain samples using the RNAqueous-4PCR Kit (Ambion) under RNase-free conditions following the manufacturer's protocol. Additional details of this method can be found in the supplementary materials.

cDNA synthesis and real-time quantitative PCR

cDNA synthesis and real-time quantitative PCR were performed as described previously.[26] Details of this method can be found in the supplementary materials.

Preparation of brain vascular lysates

Brain vascular lysates were prepared as described previously.[20] Details of this method can be found in the supplementary material.

Immunoblotting

Samples were resolved by SDS-PAGE (Bio-Rad, 10% Mini-PROTEAN TGX) and electroblotted onto nitrocellulose membrane (GE Healthcare). Additional details are provided in the supplementary material.

Antibodies

The following primary antibodies were used for immunoblotting: phospho-rpS6 (Cell Signaling, 1:1000); rpS6 (Cell Signaling, 1:1000); Actin (UBP Bio, 1:5000). The following secondary antibodies were used where appropriate: Goat anti-Mouse IgG Poly HRP (Pierce, 1:20,000); Goat-anti-Rabbit IgG Poly HRP (Pierce, 1:20,000).

Analysis of atherosclerosis

Atherosclerosis was analyzed as previously described.[27,28] Further detail is available in the supplementary material.

Non-invasive measurement of cardiopulmonary parameters

Mice were temporally anesthetized (1–4% inhaled isoflurane), and left ventricle hypertrophy was measured using the VEVO 2100 digital ultrasound microimaging system (VisualSonics) as previously described.[29]

Morris water maze

The Morris water maze[30] was used to test spatial memory as described.[20] Further detail is available in the supplementary material.

Spatial novelty

Mice were trained with three visually distinct but comparably sized objects. During testing, one object was moved to a new location within the chamber and exploration was monitored. Additional details of this task are available in the supplementary material.

Cerebral blood flow measurements

Quantitative CBF (mL/g/minute) was measured using MRI-based continuous arterial spin labeling techniques[31] as previously described[20] Briefly, measurements utilized a horizontal 7T/30 cm magnet and a 40 G/cm BGA12S gradient insert (Bruker, Billerica, MA, USA). A small circular surface coil (ID = 1.1 cm) was placed on top of the head and a circular labeling coil (ID = 0.8 cm), built into the cradle, was placed at the heart position for continuous arterial spin labeling. The two coils were positioned parallel to each other, separated by 2 cm from center to center and were actively decoupled. Paired images were acquired in an interleaved fashion with field of view = 12.8 × 12.8 mm^2, matrix = 128 × 128, slice thickness = 1 mm, 9 slices, labeling duration = 2100 ms, TR = 3000 ms, and TE = 20 ms. Continuous arterial spin labeling image analysis employed codes written in Matlab (Natick, MA, USA)[31] and STIMULATE software (University of Minnesota, Minneapolis, MN, USA) to obtain CBF.

Vascular density measurement

Magnetic resonance angiography was acquired as previously described.[20] Briefly, three-dimensional gradient-echo MR imaging with flow compensation was used with following parameters: repetition time/echo time = 26/4.3 milliseconds; field of view = 12.8 × 12.8mm^2; acquisition matrix = 128 × 128 × 192; repetition n = 4. The magnetic resonance angiography was taken before and after monocrystalline iron oxide nanoparticle (MION) injection through the tail vein (30 mg/kg) and blood vessel intensity was calculated as the change in transverse relaxivity between images. Image analysis was performed using custom-written programs (Matlab; MathWorks, Natick, MA, USA). "S-1/3"

indicates the overall MRI signal as calculated by the equation $\Delta R2/(\Delta R2^*)^{2/3}$ as described.[32]

Statistical analyses

Statistical analyses were performed using GraphPad Prism (GraphPad, San Diego, CA, USA) and included two-way ANOVA, one-way ANOVA, or Student's *t* test as appropriate, as denoted in the figure legends. All data are means ± SEM with $p < 0.05$ considered significant.

N.B. Additional methods and details of those listed above can be found in the supplementary material.

Results

Reduced phosphorylation of mTOR targets in rapamycin-treated LDLR-/- mice

To determine cardiovascular and cerebrovascular consequences of mTOR attenuation in $LDLR^{-/-}$mice, we generated four experimental cohorts (Table 1 and Methods).

Analysis of Cohort 1 samples demonstrated no significant differences in uncoagulated blood rapamycin levels in females and males (1.62 ± 0.48 ng/ml for females and 0.78 ± 0.23 ng/ml for males at 30 weeks of treatment, $p = 0.137$, Figure 1(a)). To determine whether rapamycin treatment attenuated mTOR activity in our studies, we measured rpS6 phosphorylation, a downstream target of mTOR signaling whose phosphorylation is reduced by rapamycin treatment in mouse visceral adipose tissue, heart, and brain.[21,33–35] In agreement with previous studies,[21,33,36] phosphorylation of rpS6 was significantly decreased in aortas of Cohort 1 $LDLR^{-/-}$ mice following 20 weeks of rapamycin treatment as compared to control-treated animals (Figure 1(b)). Similarly, phosphorylation of rpS6 was significantly decreased in brain vasculature of rapamycin-treated HFD-fed $LDLR^{-/-}$ animals in Cohort 4 (Figure 1(c)). No differences in mTORC2 signaling measured as phosphorylation of Akt at Ser473 were observed between rapamycin- and control-treated animals (Supplementary Figure 1).

It has been shown that rapamycin does not accumulate in liver, and that liver levels of rapamycin represent an effective proximal measure of blood levels of the drug.[37] Indeed, chronic rapamycin-supplemented HFD-feeding of Cohort 4 animals resulted in average liver rapamycin levels of 14.1 pg/mg (Figure 1(d)), which were comparable to rapamycin levels in livers of male C57BL/6 mice treated with the same chow as reported,[33,38] and correspond to 3–4 ng/ml in blood.[38] Cohorts 2 and 3 mice were not tested as these groups underwent comparable treatment to Cohort 4 mice in regards to treatment onset and duration.

Chronic mTOR attenuation decreases body weight and fat mass in aged HFD-fed LDLR−/− mice

Female, but not male HFD-fed $LDLR^{-/-}$ mice of Cohort 1 exhibited significantly lower body weight following chronic mTOR attenuation with rapamycin (Figure 2(a)) when compared to $LDLR^{-/-}$ mice fed HFD containing only eudragit, the encapsulation material for rapamycin. Both sexes showed a significant elevation in plasma triglycerides (Figure 2(a)), despite no differences in blood glucose (Figure 2(f)) nor cholesterol levels (Figure 2(g)). In spite of the observed elevation in plasma triglyceride levels, percent fat mass decreased in rapamycin-treated mice in this cohort (Figure 2(b)). Similarly, chronic mTOR attenuation in

Table 1. Animal cohorts.

	Age at start	Route and dose	Duration	Sex	Rapamycin blood levels	Measures
Cohort 1	2–2.5 months	Enteric (chow) 14 ppm	10, 20 or 30 weeks	Male and female	1.62 ng/ml (F) 0.78 ng/ml (M)	Plaque area (IHC) Ventricle mass
Cohort 2	7 months	Intraperitoneal (10 mg/kg)	16 weeks	Male	Not measured (liver rapamycin levels of 14.1 pg/mg equivalent to 3–4 ng/ml in blood)	CBF and BVD (MRI)
Cohort 3	5 months	Enteric (chow) 14 ppm	15 weeks crossover	Male and female	Not measured	Plaque area (IHC)
Cohort 4	7 months	Enteric (chow) 14 ppm	16 weeks	Male	3–4 ng/ml	Memory (NOR, MWM)

mTOR: mechanistic target of rapamycin; AD: Alzheimer's disease; LDL: low density lipoprotein; CBF: cerebral blood flow; BVD: brain vascular density; LDLR: low-density lipoprotein receptor; NO: nitric oxide; HFD: high fat diet; WT: wild type; MWM: Morris water maze; SN: spatial novelty; SAA: serum amyloid A; ApoE: apolipoprotein E; IL-6: interleukin 6.

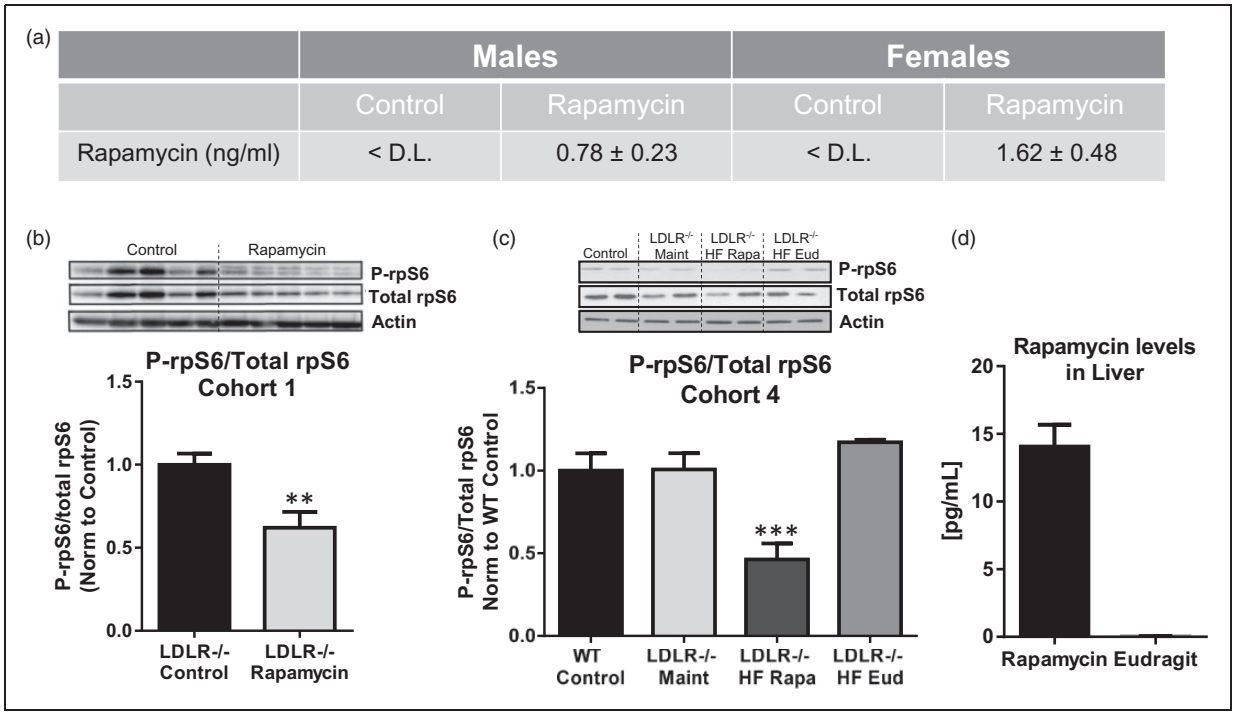

Figure 1. Chronic rapamycin treatment reduces mTOR activity in aortas and brain vasculature of LDLR$^{-/-}$ mice. (a) Blood levels of rapamycin in mice of Cohort 1 after 30 weeks of treatment. Blood levels of control-treated animals were below the detection limit (D.L.) of 0.5 ng/ml. (b) Significantly reduced phosphorylation of rpS6, a downstream target of mTOR, in aortas from rapamycin-treated animals (**, $p = 0.004$, Student's unpaired t test); (c) Significantly reduced rpS6 phosphorylation in brain vasculature purified from rapamycin-treated animals of Cohort 4 following 20 weeks of treatment (***, $F(3,12) = 12.06$, $p < 0.001$, Tukey's test on a significant effect of treatment, one-way ANOVA); (d) Rapamycin levels in liver in animals of Cohort 4. n = 8–10/group. Data are means ± SEM.

Cohort 4 mice lowered both overall body weight (Figure 2(c)) and percent fat mass (Figure 2(d)). As expected, weight gain was significantly increased in HFD-fed LDLR$^{-/-}$ mice of Cohort 4 as compared to animals on maintenance diet, with the most dramatic effects seen in the first eight weeks before reaching a stable range of body weight. Interestingly, this HFD-mediated weight gain was significantly attenuated in rapamycin-treated LDLR$^{-/-}$ mice (Figure 2(c)), suggesting that systemic attenuation of mTOR activity may inhibit fat accumulation in LDLR$^{-/-}$ mice either by changes in fat metabolism or storage.

To determine whether chronic mTOR attenuation may affect body mass composition, we performed quantitative magnetic resonance on Cohort 4 mice at 12 months of age. Whereas percent fat mass in maintenance diet-fed LDLR$^{-/-}$ mice (~25–30%) did not differ from WT, percent body fat was increased to ~45% in HFD-fed LDLR$^{-/-}$ mice (Figure 2(d)). Notably, percent body fat was significantly lower in LDLR$^{-/-}$ mice that were fed HFD supplemented with rapamycin (Figure 2(d)). With the exception of a transient initial spike in the HFD-fed groups in Cohort 4, food consumption was not significantly different amongst experimental animals regardless of diet or treatment (Figure 2(e)). Despite their significant weight gain, however, HFD-fed mice of Cohort 4, similar to those in Cohort 1 (Figure 2(a)), did not exhibit any difference in fasting glucose levels compared to either maintenance diet-fed or WT mice (Figure 2(f)) and were therefore not insulin deficient.

Chronic attenuation of mTOR does not affect hypercholesterolemia in LDLR−/− mice

LDLR$^{-/-}$ animals fed a HFD develop hypercholesterolemia.[39] Given the established effects of mTOR attenuation with rapamycin on glucose and lipid metabolism[40,41] and prior studies suggesting that rapamycin administration results in hypercholesterolemia,[42] we investigated the effects of rapamycin treatment on circulating cholesterol levels in HFD-fed LDLR$^{-/-}$ mice. Since LDLR is responsible for clearing LDL cholesterol from the periphery, it was not surprising that LDL cholesterol levels were significantly higher in LDLR$^{-/-}$ mice compared to WT. Notably, serum LDL cholesterol levels were comparable between all LDLR$^{-/-}$ mice regardless of diet or treatment (Figure 2(g)), suggesting that HFD does not confer any further cholesterol burden at this age. Similarly,

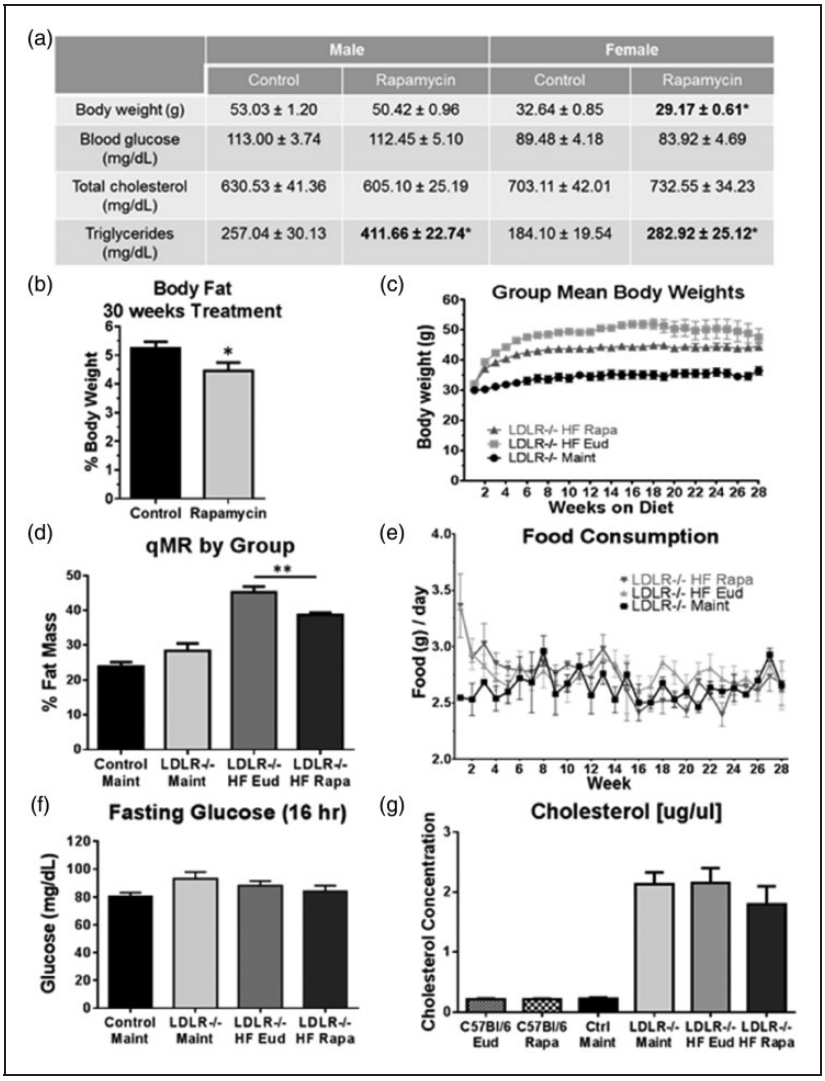

Figure 2. Chronic mTOR attenuation reduces body weight and fat mass gains in HFD-fed LDLR$^{-/-}$ mice. (a) Decreased body weight despite a significant increase in blood triglycerides without changes in glucose or cholesterol in rapamycin-treated HFD-fed LDLR$^{-/-}$ mice of Cohort 1; (b) Reduced body fat in rapamycin-treated HFD-fed LDLR$^{-/-}$ mice of Cohort 1 (*, $p = 0.0465$, Student's unpaired t test); (c) Weight gain in Cohort 4 HFD- two-way ANOVA); (d) Reduced body fat in rapamycin-treated LDLR$^{-/-}$ mice of Cohort 4 (**, $F(3, 42) = 38.54$, $p < 0.0001$, Tukey's test on a significant effect of treatment, one-way ANOVA); No differences in food consumption (e) or fasting glucose (f) levels were observed among experimental groups; (g) Significant increases in blood cholesterol following HFD feeding in Cohort 4 were unaffected by rapamycin treatment. n = 11–15/group (males) and n = 13–16/group (females) for (a–b) and n = 10/group (c–f). Data are means ± SEM.

rapamycin treatment had no effect on cholesterol levels in WT C57BL/6 J.

Chronic mTOR attenuation reduces atherosclerotic lesion area in the aortic arch

Previous studies[18,43] have suggested that mTOR has a role in atherogenesis. To determine whether chronic mTOR attenuation affected the development of atherosclerotic lesions in HFD-fed LDLR$^{-/-}$ groups, we measured aortic arch lesion area using both a time-course (Cohort 1) and a crossover design (Cohort 3, Methods and Table 1). Aortic arch lesion area in HFD-fed LDLR$^{-/-}$ mice was significantly reduced 20 and 30 weeks after initiation of rapamycin treatment in both male and female mice of Cohort 1 (Figure 3(a)).

Interestingly, lesion areas in the aortic root were reduced only in female mice of Cohort 3 that had been switched from control to rapamycin diet (Figure 3(b)), suggesting that mTOR has a role in development, but not in the initiation, of plaque deposition during atherogenesis in female mice. Notably, left ventricle

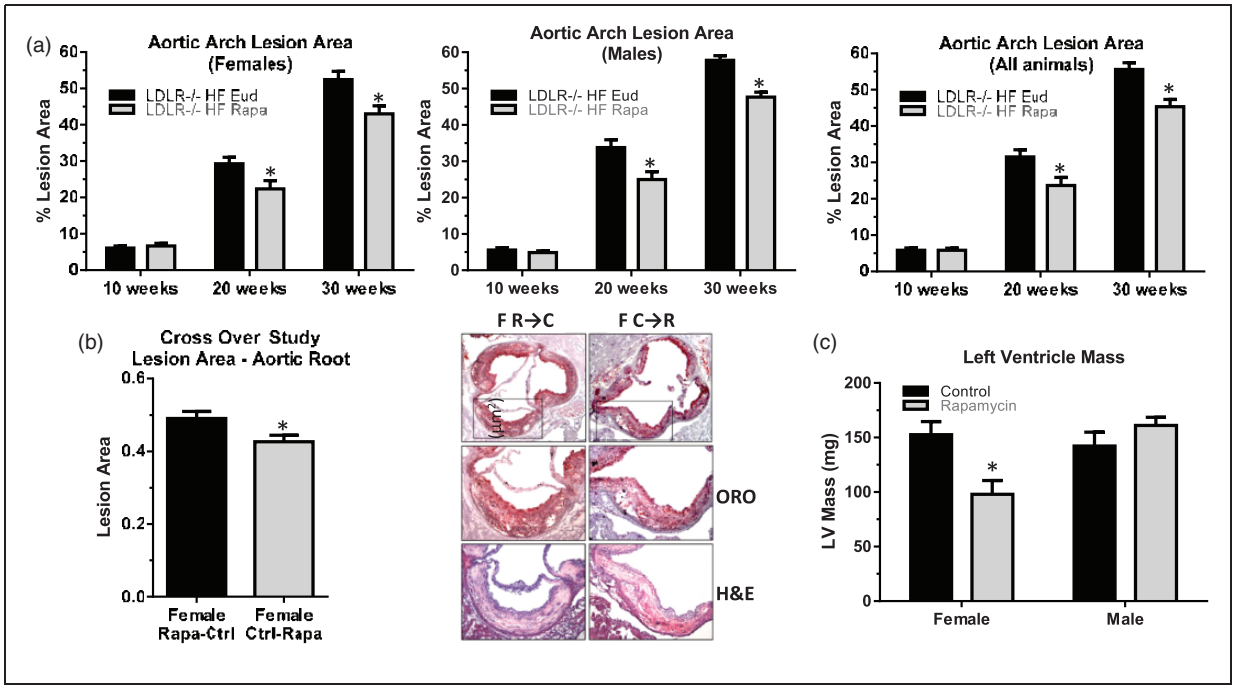

Figure 3. Reduced atherosclerotic lesion size in the aortic arch following mTOR attenuation. Overall aortic arch lesion area (a) in HFD-fed LDLR$^{-/-}$ female (left panel), male (center panel) and both female and male (right panel) mice were significantly reduced following either 20 or 30 weeks of rapamycin treatment (*, two-way ANOVA $F(1,34) = 11.69$, $p = 0.002$) n = 6–8/group; (b) Reduced lesion area by rapamycin treatment in the aortic root of female mice after, but not prior to, the onset of lesion formation (left panel, quantitative analyses of anatomical data; right panel, representative images (oil red o (ORO), haemotoxylin and eosin (H&E)). Student's unpaired *t* test, *, $p = 0.026$), n = 12/group (c) No difference in male but significantly reduced left ventricle mass in female LDLR$^{-/-}$ mice treated with rapamycin (*, two-way ANOVA $F(1,28) = 10.30$, $p = 0.029$), n = 8/group. Data are means ± SEM.

hypertrophy was significantly reduced in females, but not in males (data not shown) after 30 weeks of rapamycin treatment (Figure 3(c)). Measured ejection fraction values were indistinguishable from WT for both male and female animals (data not shown), though the sample size of these studies was likely too small to detect differences in these in vivo measures of cardiac function.

Cerebrovascular rarefaction and cerebral hypoperfusion are reduced by mTOR attenuation

We used arterial spin labeling magnetic resonance imaging to measure CBF and MRI-based angiography to estimate BVD. CBF was significantly decreased in LDLR$^{-/-}$ mice; this deficit was exacerbated by HFD (Figure 4(a)). Because relatively small groups provide sufficient statistical power in MRI studies (see Methods), we were able to include a maintenance diet-fed LDLR$^{-/-}$ group that was treated with rapamycin in these experiments. Notably, chronic mTOR attenuation by intraperitoneal rapamycin administration restored CBF in maintenance diet-fed LDLR$^{-/-}$ mice to levels comparable to WT mice, suggesting that mTOR has a critical mechanistic role in brain hypoperfusion in LDLR$^{-/-}$ animals. The consequences of mTOR attenuation by rapamycin on CBF in HFD-fed LDLR$^{-/-}$ mice could not be unequivocally determined due to accelerated weight loss and high mortality in this group, in agreement with the observed rapamycin-mediated reduction in body weight in HFD-fed LDLR$^{-/-}$ (Figure 2(c)). Of note, and although this observation can only be considered anecdotal, a single surviving rapamycin-treated HFD-fed LDLR$^{-/-}$ animal (n = 1) exhibited CBF levels indistinguishable from those of WT control mice (Figure 4(a)). To determine whether differences in CBF between control- and rapamycin-treated LDLR$^{-/-}$ mice could be explained by changes in BVD as previously shown for hAPP(J20) mice modeling AD,[20] we measured BVD using MRI-based angiography. Indeed, we found decreased CBF in LDLR$^{-/-}$ was accompanied by proportionate differences in BVD (Figure 4(b) and (c)), suggesting that the preservation of BVD may underlie the restoration of CBF in rapamycin-treated LDLR$^{-/-}$ mice.

Chronic mTOR attenuation improves memory in LDLR−/− mice

Decreased CBF is associated with cognitive dysfunction.[13,44,45] To determine whether decreased CBF

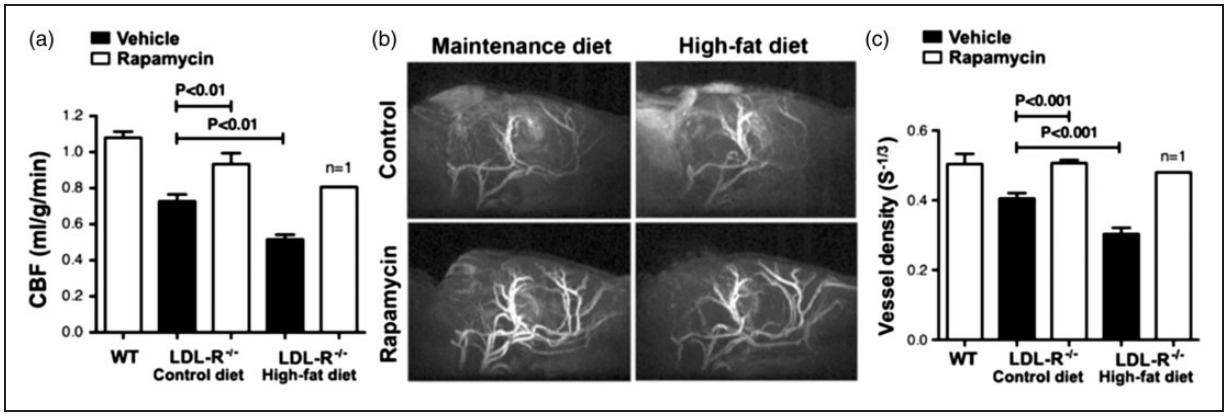

Figure 4. Restored cerebral blood flow and preserved brain vascular density by mTOR attenuation in LDLR$^{-/-}$ mice. (a) Profound CBF deficits in 12 month old LDLR$^{-/-}$ mice were restored to levels indistinguishable from those of WT mice as a result of chronic rapamycin treatment ($F(2,7) = 21.22$, $p = 0.001$, Tukey's test, one-way ANOVA); (b–c) Reduced BVD (calculated as $S = \Delta R2/(\Delta R2^*)^{2/3}$) in control-treated but not in rapamycin-treated LDLR$^{-/-}$ mice ($F(2,7) = 41.48$, $p = 0.0001$, Tukey's test, one-way ANOVA; (b) Representative MRI angiograms; (c) Quantitative analyses of angiogram data. n = 3–4. Data are means ± SEM. N.B. Data for the single surviving HFD-fed rapamycin-treated LDLR$^{-/-}$ animal are provided (a,c) but were not included in the ANOVA. Values for WT CBF (a) and BVD (c) are included as a reference and correspond to measures performed on separate groups of WT C57Bl/6J mice of comparable age; these values were not included in the ANOVA.

resulted in impaired cognitive function in LDLR$^{-/-}$ mice and ascertain the role of mTOR, we next assessed recognition memory in LDLR$^{-/-}$ mice of Cohort 4 using the spatial novelty (SN) paradigm, a simple discrimination task which requires that the animals retain the prior locations of objects presented in the experimental arena and thus recognize novel object placement. All animals explored the three objects presented during training equally (Figure 5(a)), ruling out potential confounds arising from aversion/preference for a particular object or location. During testing, WT and maintenance diet-fed LDLR$^{-/-}$ animals preferentially explored the object that had been moved (Figure 5(b)), indicating retention of the object's prior location. HFD-fed LDLR$^{-/-}$ mice, however, spent an equivalent percent of trial time examining each of the three objects (Figure 5(b)), indicating a deficit in retention of the prior location of the displaced object. Notably, rapamycin-treated HFD-fed LDLR$^{-/-}$ mice performed indistinguishably from WT mice, suggesting that attenuation of mTOR activity restores hippocampus-dependent recognition memory in HFD-fed LDLR$^{-/-}$ mice.

To rule out potential task-specific effects of mTOR attenuation by rapamycin and define whether the observed improvement in SN recognition in rapamycin-treated HFD-fed LDLR$^{-/-}$ mice was associated with improvements of other aspects of context-related learning and memory, we used the Morris water maze (MWM). MWM design limits the number of animals that can be included in an experiment to 60 due to time constraints inherent with keeping time-at-testing as constant as possible. For our studies, n = 60 corresponded to 4 groups of 15 animals each to have sufficient power to detect meaningful differences between group means (Methods). Because HFD-fed LDLR$^{-/-}$ are the established model of atherosclerosis, we chose the four groups to be included in these studies to be (1) maintenance-fed WT controls; (2) maintenance-fed LDLR$^{-/-}$ mice; (3) control-treated (eudragit) HFD-fed LDLR$^{-/-}$ and (4) rapamycin-treated, HFD-fed LDLR$^{-/-}$ mice in order to identify effects of mTOR attenuation on cognitive and brain vascular functional outcomes in HFD-fed LDLR$^{-/-}$ mice.

This behavioral task requires intact hippocampal function similarly to SN, but requires processing of more complex sets of spatial information to learn a specific location. As expected, spatial learning in the MWM progressively improved across four days of training for WT mice (Figure 5(c)). Performance of both HFD and maintenance diet-fed LDLR$^{-/-}$ mice, however, was significantly impaired on training days 2 and 3 (Figure 5(c)). Increased latencies in LDLR$^{-/-}$ mice fed a maintenance diet suggested delayed spatial learning in this group, a finding in contrast to their ability to retain simple contextual information (Figure 5(b)).

Distance swam can provide a better measure of performance when swimming speeds are significantly different amongst groups. We report no differences between experimental groups for distance swam (Figure 5(d)), but because reduced swimming speed of HFD-fed LDLR$^{-/-}$ during training (Figure 5(e)) was a consequence of increased floating (Figure 5(f)),

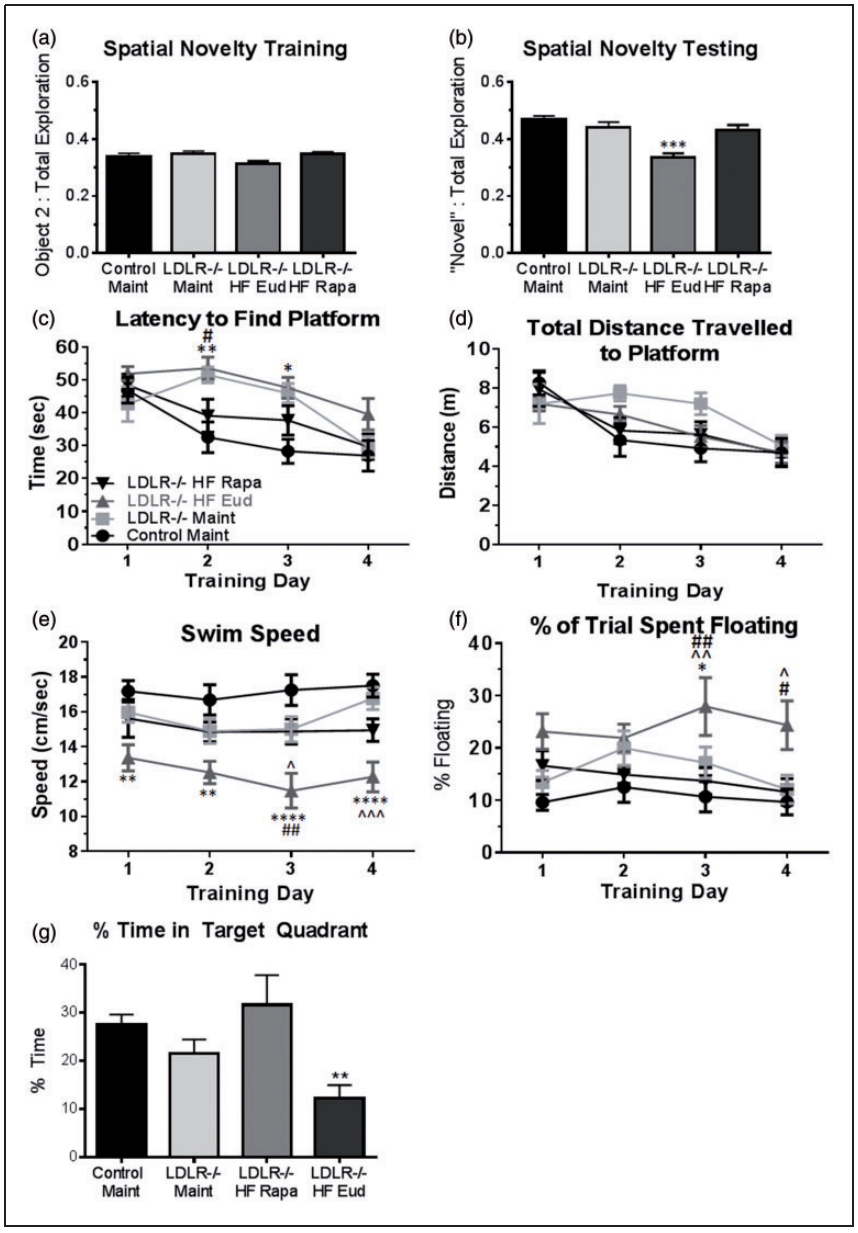

Figure 5. Rapamycin treatment abolishes memory impairments in LDLR$^{-/-}$ mice. (a) No differences among experimental groups during training in the spatial novelty task; (b) Recognition memory in rapamycin-treated HFD-fed LDLR$^{-/-}$ mice is restored to levels indistinguishable from those of WT mice ($F(3, 35) = 7.048$, $p = 0.0008$ Tukey's test, one-way ANOVA), n = 10–11/group; (c) Improved performance in rapamycin-treated HFD-fed mice, but not in in control-treated LDLR$^{-/-}$ mice fed either HFD or maintenance chow in days 2 and 3 of training in the MWM [($F(3, 35) = 6.336$, $p = 0.0015$) and training day ($F(3, 105) = 15.19$, $p < 0.0001$, Tukey's test, RM two-way ANOVA]. Although all groups swam comparable distances during training days, distances swam were artificially decreased in untreated HFD-fed LDLR$^{-/-}$ mice (d) due to a significant reduction in swimming speed (e) ($F(3, 35) = 10.71$, $p < 0.0001$, Tukey's test, RM two-way ANOVA) as a result of increased floating (f) ($F(3, 35) = 4.87$, $p = 0.006$, Tukey's test, RM two-way ANOVA). n = 10/group. Data are means ± SEM. (g) HFD-fed LDLR$^{-/-}$ mice exhibit significant cognitive impairment during the probe trial in which the platform is removed. Rapamycin treatment restored exploration in the appropriate quadrant to WT levels (**, one-way ANOVA, $p = 0.013$). *, HFD-fed LDLR$^{-/-}$ different from Control Maint; ^, HFD-fed LDLR$^{-/-}$ different from Maint-fed LDLR$^{-/-}$; #, HFD-fed LDLR$^{-/-}$ different from rapa-fed LDLR$^{-/-}$ mice.

conclusions on spatial learning could not be unequivocally drawn for this group. Performance of rapamycin-treated HFD-fed LDLR$^{-/-}$ mice, in contrast, was not confounded by decreases in swimming speed nor floating (Figure 5(e) and (f)) and was indistinguishable from that of WT control mice (Figure 5(c)), suggesting that attenuation of mTOR activity abrogates spatial learning defects in HFD-fed LDLR$^{-/-}$ mice. All experimental groups performed comparably on day 4 of training, indicating that spatial learning is impaired but not abolished in LDLR$^{-/-}$ mice. Furthermore, HFD-fed LDLR$^{-/-}$ control (eudragit) mice exhibited a statistically significant deficit in percent time spent in the target quadrant during the probe trial (Figure 5(g)) compared to all other groups, whereas rapamycin-treated subjects were indistinguishable from the WT group. All experimental animals were confirmed to possess comparable motor and neurological competency prior to behavioral testing. Percent time engaged in thigmotaxis could not be used as a proximal measure of evoked anxiety because of increased floating, which confounds this measure.

mTOR attenuation suppresses markers of brain and systemic inflammation in LDLR-/- mice

Because a high systemic inflammatory state has been implicated in the pathogenesis of atherosclerosis in LDLR$^{-/-}$ mice[46] as well as in the etiology of cognitive impairment in vascular dementia,[47] we investigated whether improved cardiovascular and neurovascular measures in LDLR$^{-/-}$ mice as a result of mTOR attenuation with rapamycin were associated with reduced brain and systemic inflammation. To test this hypothesis, we measured levels of the pro-inflammatory cytokine IL-6 and of serum amyloid A (SAA) as markers of inflammation in brain and in serum, respectively, of Cohort 4 LDLR$^{-/-}$ mice. Rapamycin treatment conferred a notable reduction in whole brain levels of IL-6 in HFD-fed LDLR$^{-/-}$ mice, though this trend did not reach statistical significance due to high variability in the control-treated group (Figure 6(a)). Of note, variance was significantly lower in the rapamycin-treated group, suggesting that attenuation of mTOR may exert a regulatory effect over brain IL-6 levels that our studies were not sufficiently powered to detect.

We next examined serum levels of SAA, a family of apolipoproteins secreted during acute inflammation, as a measure of systemic inflammatory state in all experimental groups. SAA was significantly elevated in sera of HFD-fed LDLR$^{-/-}$ mice as compared to either maintenance diet-fed LDLR$^{-/-}$ mice or WT control animals (Figure 6(b)). Rapamycin treatment, in contrast, conferred a significant reduction in SAA in HFD-fed LDLR$^{-/-}$ mice.

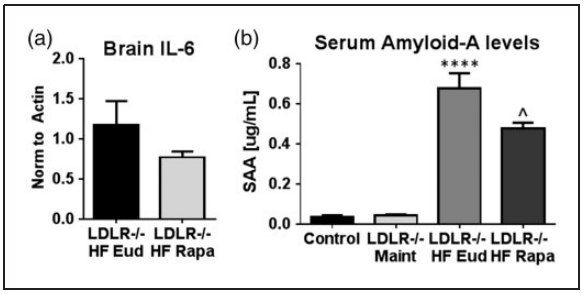

Figure 6. Chronic rapamycin treatment abrogates an increase in markers of systemic inflammation in LDLR$^{-/-}$ mice. (a) Reduced brain IL-6 levels in rapamycin-treated HFD-fed LDLR$^{-/-}$ mice as compared to control-treated HFD-fed LDLR$^{-/-}$ mice [$p = 0.2566$, Student's unpaired t test with Welch's correction. Variance was significantly different among groups ($p = 0.001$, $F(4, 6) = 12.09$], n = 5–7/group); (b) Increased serum levels of SAA in control HFD-fed LDLR$^{-/-}$ mice as compared to maintenance-fed LDLR$^{-/-}$ are attenuated by rapamycin treatment (****$p < 0.0001$, $F(3, 15) = 49.79$, Tukey's test, one-way ANOVA and $p = 0.028$, Student's unpaired t test). n = 6/group Data are means ± SEM.

Discussion

Rapamycin treatment significantly reduced mTOR activity in our studies (Figure 1(b) and (c)), despite blood levels that were lower than the 3–4 ng/ml reported by both Zhang et al.[33] and Fischer et al.[48] Of note, however, the mice in those studies were in the C57BL/6 and C57BL/6 J backgrounds, respectively, which may explain the differences in rapamycin blood levels observed. As previously reported,[18,19] we showed that chronic rapamycin-mediated mTOR attenuation decreased lesion area in the aortic arch of HFD-fed LDLR$^{-/-}$ mice (Figures 2 and 3) despite pronounced hypercholesterolemia. While some studies in either transplant patients[49,50] or the LDLR$^{-/-}$ model reported an increase in LDL cholesterol following mTOR attenuation,[51] in our studies, chronic mTOR attenuation did not change cholesterol levels in blood (Figure 2(g)). Thus, body weight and body mass composition changes observed in rapamycin-treated HFD-fed LDLR$^{-/-}$ mice cannot be attributed to alterations in cholesterol metabolism. Still, the observation that rapamycin treatment increases triglyceride levels (Figure 2(a)) is consistent with reports of dyslipidemia in human transplant[49] and cancer[42] patients treated with mTOR inhibitors. All mice in our experiments exhibited levels of LDL cholesterol within expected ranges.[52] Thus, it is possible that treatment with rapamycin, as in the present studies, has different consequences for overall blood cholesterol levels than everolimus, the rapamycin derivative used by Mueller et al.[51] Alternatively, there may exist a 'ceiling' effect where LDL cholesterol levels are maximal in LDLR$^{-/-}$

mice due to their inability to clear it from their circulation.

Furthermore, we report differences in body weight and in parameters of lipid metabolism between our mouse cohorts (Figure 2) which may arise from differences in age at initiation of treatment (2–2.5 and 7 months of age for Cohort 1 and Cohort 4, respectively). Our data suggest that chronic systemic attenuation of mTOR activity by enteric delivery of rapamycin may have distinct effects on both triglyceride levels and overall body weight depending on whether mice have completed development or are still developing key metabolic organs/tissues such as skeletal muscle. It is also conceivable that a body weight effect was not observed in the younger cohort (Cohort 1) simply because they had not yet begun storing excess body fat as a consequence of age-associated slowing of their metabolism. Still, our observation that rapamycin treatment conferred no differences in fasting glucose levels (Figure 2(f)) in HFD-fed LDLR$^{-/-}$ mice suggests that reduced body weight in this group (Figure 2(a) and (c)) may result from decreased body fat (Figure 2(b) and (d)) and further suggests that chronic attenuation of mTOR may reduce fat synthesis and/or accumulation in HFD-fed LDLR$^{-/-}$ mice.

It has been proposed that rapamycin-mediated suppression of mTOR activity, and the resulting decrease in cellular proliferation and increase in autophagy, may inhibit atherosclerotic plaque growth and destabilization[53] and thereby limit cardiovascular damage associated with increasing levels of LDL cholesterol. Though the present study did not directly address either of these mechanisms, prior studies indicate a role of mTOR in increasing macrophage numbers associated with atherosclerotic plaques[54] and in promoting the transition from early macrophage-enriched lesions to advanced plaques.[51] Conversely, Peng et al.[55] suggested that the development of atherosclerosis is restricted by mTOR. Here, we observed that rapamycin treatment significantly decreased aortic lesion area in LDLR$^{-/-}$ mice (Figure 3(a)), in agreement with previous studies showing that everolimus reduced atherosclerotic lesion size and composition.[51] Similar findings of rapamycin-mediated reduction in aortic lesion area and plaque formation in HFD-fed ApoE$^{-/-}$ mice have also been reported.[19,56] Of note, chronic mTOR attenuation inhibited left ventricle hypertrophy in female but not male HFD-fed LDLR$^{-/-}$ mice (Figure 3(c)), in agreement with recent studies from the laboratory of Dr. Peter Rabinovitch that demonstrated that rapamycin treatment improved diastolic function in female mice[57] through a mechanism involving the transient induction of autophagy and mitogenesis. These studies as well as our data are consistent with the larger effects of mTORC1 attenuation by rapamycin in murine aging.[21] Although no other sex-specific dimorphisms were observed in our studies, the sex-specific differences observed in left ventricle hypertrophy in HFD-fed LDLR$^{-/-}$ animals are in accordance with those in the magnitude of lifespan extension by systemic mTOR attenuation, which is larger in female than in male mice.[21,33]

Our crossover studies (Cohort 3) suggested that mTOR has a role in the development, but not in the early steps of plaque formation (Figure 3(b)). Thus, mTOR attenuation may be more effective in the treatment rather than in the prevention of atherosclerosis. While hypercholesterolemia in LDLR$^{-/-}$ mice was not affected by rapamycin, both body weight and percent body fat in HFD-fed LDLR$^{-/-}$ animals were significantly reduced (Figure 3(a) to (c)), suggesting that mTOR activity is required for fat accumulation in LDLR$^{-/-}$ mice. This finding is consistent with previous reports of lowered body weight in WT mice treated with everolimus[51] and in rats injected with rapamycin,[58] and thus may be generalizable and not mechanistically related to LDLR genotype.

Numerous studies have reported that systemic mTOR attenuation by rapamycin leads to dose- and treatment duration-dependent hyperlipidemia.[50,59] The majority of these studies, however, have investigated relatively short term (<6 weeks) rapamycin treatment in human subjects. Recent studies by Fang et al.[60] showed that while short-term (6 weeks) treatment of genetically heterogeneous mice resulted in hyperlipidemia, long-term (up to 20 weeks) rapamycin treatment actually improved lipid profiles as compared to control-treated groups.[60] Our studies, however, documented significantly increased triglyceride levels in both male and female LDLR$^{-/-}$ mice following 30 weeks of rapamycin treatment (Figure 3(a)). This difference may be explained by the difference in genetic background between the mice used by Fang et al. and the LDLR$^{-/-}$ animals in our studies. Alternatively, it is possible that the differences observed in the response to long-term rapamycin treatment may be at least partially due to a requirement for LDLR in the metabolic adaptation of mice to long-term mTOR attenuation.[60] Because our LDLR$^{-/-}$ cohorts were also fed HFD, it is possible that exacerbated dyslipidemia increased adipogenesis or the activation of fat storage mechanisms. Of note, Polak et al.[61] showed that mTORC1 is required for adipogenesis, as knockdown of Raptor results in decreased adipose tissue and reduced obesity in mice, supporting the hypothesis that weight reduction following chronic mTOR attenuation with rapamycin may be due to a reduction in fat synthesis rather than to increased adipolysis.

Remarkably, intraperitoneal rapamycin treatment, more so than the enteric route, induced significant weight loss and premature death in LDLR$^{-/-}$ mice

fed HFD (Figure 4). This is dissimilar to recent studies by Johnson et al.[22,62] in which IP administration of rapamycin at similar or much higher doses than those used in our studies extended lifespan by attenuating disease symptoms in the Ndufs4 knockout mouse model of Leigh Syndrome. In light of these data, and the observation that intraperitoneal rapamycin did not result in any observable toxicity in maintenance-fed $LDLR^{-/-}$ mice, our studies suggest that wasting and death in severely dyslipidemic HFD-fed $LDLR^{-/-}$ mice may have been caused by bouts of exacerbated metabolic imbalance associated with intraperitoneal rapamycin administration.

Cardiovascular disease risk factors increase risk for AD and vascular dementia (reviewed in Luchsinger and Mayeux[63] and de Bruijn and Ikram[64]); thus, effective management of these risk factors is recommended to prevent cognitive decline/dementia.[65] Our previous studies demonstrated that attenuation of mTOR activity both before[34] and after[20] onset of cognitive impairments abolished AD-like cognitive deficits and negated profound deficits in brain vascular integrity and function in AD-model mice.[20] Given that $LDLR^{-/-}$ mice develop vascular pathology that affects brain microvasculature,[66] we hypothesized that mTOR-driven mechanisms of neurovascular dysfunction may contribute to cognitive impairment associated with atherosclerosis in $LDLR^{-/-}$ mice that have elevated cholesterol and develop atherosclerosis even when fed a maintenance diet.[67] Our MRI and MRA studies revealed that brain hypo-perfusion (Figure 4(a)) could be explained by a decrease in BVD (Figure 4(b) and (c)), potentially as a consequence of increased systemic and brain inflammation (Figure 6) following hyperlipidemia. These deficits occurred regardless of diet but were exacerbated though HFD feeding. Thus, dyslipidemia in $LDLR^{-/-}$ mice is associated with profound neurovascular disintegration and dysfunction that is proportional to the severity of the imbalance. In agreement with our hypothesis, attenuation of mTOR by rapamycin appeared to negate neurovascular dysfunction and damage in $LDLR^{-/-}$ mice, although these data represent a single observation in the only surviving subject in the HFD-fed, rapamycin-treated $LDLR^{-/-}$ group. Still, these data may hint at a role of mTOR-dependent mechanisms of vascular dysfunction upstream of HFD-triggered pathways of exacerbated dyslipidemia and atherogenesis.

Our recent studies in mice modeling AD[20] suggested a model in which age-associated mTOR-dependent loss of neurovascular integrity and function is an apical mechanism of pathogenesis in AD. Because mTOR drives murine aging,[68] we hypothesized that mTOR-dependent loss of neurovascular integrity and function may contribute to the pathogenesis of other neurological diseases of aging such as cognitive impairment associated with atherosclerosis. This model predicts that the restoration of neurovascular function by mTOR attenuation would lead to improved cognitive function in $LDLR^{-/-}$ mice.[63,64] As expected from observed profound CBF and BVD deficits (Figure 4), spatial learning in $LDLR^{-/-}$ mice was poor and in the HFD-fed group was confounded by high levels of floating, reflecting increased helplessness in response to the highly anxiogenic environment of the MWM. Further, because performance in MWM depends on unencumbered swimming, increased floating in HFD-fed $LDLR^{-/-}$ mice as training progressed may have been exacerbated by physical limitations such as obesity, which changes the area-body weight ratio and thereby the dynamics of swimming, and decreased endurance due to cardiovascular deficits. All experimental animals were confirmed to possess comparable motor and neurological competency prior to behavioral testing. Thus, the observed increase in floating in HFD-fed $LDLR^{-/-}$ mice (Figure 5(f)) can be explained by increased helplessness in response to the anxiogenic environment of the MWM. Percent time spent in thigmotaxic swim could not be used as a proximal measure of evoked anxiety because increased floating confounded this measure. Of note, rapamycin treatment was sufficient to alleviate increased helplessness in HFD-fed $LDLR^{-/-}$ mice (Figure 5(f)), which may have contributed to improved performance in this task. These findings are consistent with prior studies suggesting anxiolytic and anti-depressive[35,69] effects of systemic mTOR attenuation.

Because of significantly increased floating (Figure 5(f)), MWM data for the HFD-fed group could not be unequivocally interpreted, but a delay in spatial learning in maintenance chow-fed $LDLR^{-/-}$ animals (Figure 5(c)), that still develop atherosclerosis, albeit at a slower pace than HFD-fed animals, suggests that vascular consequences of dyslipidemia in $LDLR^{-/-}$ mice may be sufficient to impair spatial learning. Learning in rapamycin-treated HFD-fed $LDLR^{-/-}$ mice, however, was indistinguishable from that of WT mice, indicating that learning deficits in $LDLR^{-/-}$ mice could be abrogated by chronic mTOR attenuation. Furthermore, HFD-fed mice exhibited significant deficits in the probe trial, which measures retention of spatial information acquired during training, that were restored by chronic rapamycin treatment (Figure 5(g)), suggesting that reduction of mTOR activity may confer improvements to spatial memory function in HFD-fed $LDLR^{-/-}$ mice.

In addition to spatial learning deficits, our studies revealed significant contextual recognition memory deficits as measured with the SN task that were abrogated by chronic attenuation of mTOR activity by

rapamycin, rendering HFD-fed LDLR$^{-/-}$ mice functionally indistinguishable from WT mice (Figure 5(b)). Taken together, our data indicate that systemic inhibition of mTOR restores spatial learning and contextual memory as measures of cognitive function in HFD-fed LDLR$^{-/-}$ mice. Of note, although LDLR$^{-/-}$ mice fed a maintenance diet showed profound CBF deficits that may have been exacerbated by HFD (Figure 4) and resulted in spatial learning impairment (Figure 5(c)) they did not show deficits in the minimally anxiogenic SN task which measures retention of contextual information but does not require encoding of spatial information using distal environmental cues as in the MWM. Conversely, the exacerbation of learning and recognition memory deficits resulting from feeding a HFD was not proportional to the magnitude of CBF and BVD deficits in HFD-fed LDLR$^{-/-}$ mice (Figure 5).

Recent studies established a critical role for inflammation in the etiology of atherosclerosis and demonstrated the involvement of inflammatory mediators at all stages of disease.[70,71] Interestingly, both pro- and anti-inflammatory roles of mTOR have been described in various diseases.[72,73] Our studies showed that systemic mTOR attenuation by rapamycin decreased serum SAA levels and also reduced variability and tended to decrease overall levels of IL-6 in brain (Figure 6), suggesting that mTOR attenuation lessens systemic and potentially also brain inflammation. Members of the SAA family that are induced by inflammation have previously been shown to degrade extracellular matrix, potentially through the induction of matrix metalloproteinase 9.[74] Thus, decreasing levels of SAA through mTOR attenuation may be a mechanism by which rapamycin treatment restores vascular integrity and function both in brain as well as in the periphery in HFD-fed LDLR$^{-/-}$ mice. Furthermore, reduced inflammation in LDLR$^{-/-}$ mice may explain the overall reduction in aortic lesion size following rapamycin treatment despite the lack of discernible effects of treatment on serum cholesterol levels. Increased systemic inflammation cannot explain the observed brain vascular damage and dysfunction in LDLR$^{-/-}$ mice fed maintenance chow, however, since SAA was not increased in this group. Still, while our findings here suggest a correlation between cardiovascular health and inflammation, further mechanistic studies are necessary to identify the mechanistic role of mTOR on this relationship.

In conclusion, our studies show that LDLR$^{-/-}$ mice develop profound neurovascular deficits (Figure 4) that negatively impact cognitive function as well as non-cognitive components of behavior (Figure 5). Thus, in addition to cardiovascular disease, LDLR$^{-/-}$ mice may have significant potential as a model of vascular dementia. Further, our data suggest that mTOR activity underlies neurovascular dysfunction and cognitive deficits in LDLR$^{-/-}$ mice, and that chronic mTOR attenuation with rapamycin is sufficient to restore these deficits. Remarkably, learning and memory impairments in Cohort 4 LDLR$^{-/-}$ mice (Figure 5) correlated with both the severity of neurovascular damage (Figure 4) and the observed magnitude of peripheral atherogenic processes (Figure 3) in similarly-treated subjects from Cohorts 2 and 1, respectively. Our findings of both improved cognitive outcomes and improved cardiovascular health following mTOR attenuation suggests that cardiovascular and cognitive benefits of rapamycin administration may be at least partially mediated through common mechanisms of decreased inflammation (Figure 6), and potentially, preserved endothelial function.[20]

The experiments reported confirm a role of mTOR in mechanisms of neurovascular and cardiovascular dysfunction associated with dyslipidemia and atherosclerosis in LDLR$^{-/-}$ mice. While other studies have suggested that LDLR$^{-/-}$ mice exhibit cognitive dysfunction,[16,17] to our knowledge, mTOR attenuation by chronic rapamycin is the first successful intervention to counteract these deficits. That rapamycin treatment restored vascular integrity and function and was also associated with cognitive rescue indicates a critical role of mTOR-mediated neurovascular dysfunction as an initiator of age-associated cognitive impairment rather than as an indirect consequence of ongoing pathology. Considering the established relationship between cardiovascular disease and risk for future dementia,[63,64] mTOR attenuation with rapamycin may represent a viable intervention for age-related cognitive disorders, including but not limited to cognitive dysfunction associated with atherosclerosis.

Funding

The author(s) disclosed receipt of the following financial support for the research, authorship, and/or publication of this article: These studies were supported by a William & Ella Owens Medical Research Foundation Grant, an NIH Institute for Integration of Medicine and Science Award and in part by Merit Review Award I01 BX002211-01A2 to VG from the United States (U.S.) Department of Veterans Affairs, Biomedical Laboratory Research and Development Service. JBJ and CVS are supported by NIA Training Grant T32AG021890. ALL is supported by K01AG040164. We recognize the support of the San Antonio Nathan Shock Center of Excellence in the Biology of Aging (2 P30 AG013319-21), the San Antonio Medical Foundation, the JMR Barker Foundation, and generous support from the Robert L. Bailey and daughter Lisa K. Bailey Alzheimer's Fund in memory of Jo Nell Bailey.

Declaration of conflicting interests

The author(s) declared no potential conflicts of interest with respect to the research, authorship, and/or publication of this article.

Authors' contributions

Experiments were designed by JBJ, ALL, MG, MJ, RA, and VG and performed by JBJ, ALL, ND, SH, CVS, MG, MJ, QZ, LAM, ML. Manuscript was written by JBJ and VG and edited by JBJ, ALL, RA, and VG.

Supplementary material

Supplementary material for this paper can be found at the journal website: http://journals.sagepub.com/home/jcb

References

1. Morris JC. Early-stage and preclinical Alzheimer disease. *Alzheimer Dis Assoc Disord* 2005; 19: 163–165.
2. Breteler MM, Claus JJ, Grobbee DE, et al. Cardiovascular disease and distribution of cognitive function in elderly people: the Rotterdam Study. *BMJ* 1994; 308: 1604–1608.
3. Kuller LH, Shemanski L, Manolio T, et al. Relationship between ApoE, MRI findings, and cognitive function in the Cardiovascular Health Study. *Stroke* 1998; 29: 388–398.
4. Kivipelto M, Ngandu T, Fratiglioni L, et al. Obesity and vascular risk factors at midlife and the risk of dementia and Alzheimer disease. *Arch Neurol* 2005; 62: 1556–1560.
5. Zlokovic BV. Neurovascular pathways to neurodegeneration in Alzheimer's disease and other disorders. *Nat Rev Neurosci* 2011; 12: 723–738.
6. Voss MW, Nagamatsu LS, Liu-Ambrose T, et al. Exercise, brain, and cognition across the life span. *J Appl Physiol* 2011; 111: 1505–1513.
7. Hillman CH, Erickson KI and Kramer AF. Be smart, exercise your heart: exercise effects on brain and cognition. *Nat Rev Neurosci* 2008; 9: 58–65.
8. McAuley E, Szabo AN, Mailey EL, et al. Non-Exercise estimated cardiorespiratory fitness: associations with brain structure, cognition, and memory complaints in older adults. *Mental Health Phys Act* 2011; 4: 5–11.
9. Jousilahti P, Vartiainen E, Tuomilehto J, et al. Sex, age, cardiovascular risk factors, and coronary heart disease: a prospective follow-up study of 14 786 middle-aged men and women in Finland. *Circulation* 1999; 99: 1165–1172.
10. Herrmann W and Knapp JP. Hyperhomocysteinemia: a new risk factor for degenerative diseases. *Clin Lab* 2002; 48: 471–481.
11. Rojo L, Sjoberg MK, Hernandez P, et al. Roles of cholesterol and lipids in the etiopathogenesis of Alzheimer's disease. *J Biomed Biotechnol* 2006; 2006: 73976.
12. Sharrett AR, Ding J, Criqui MH, et al. Smoking, diabetes, and blood cholesterol differ in their associations with subclinical atherosclerosis: the Multiethnic Study of Atherosclerosis (MESA). *Atherosclerosis* 2006; 186: 441–447.
13. Gorelick PB, Scuteri A, Black SE, et al. Vascular contributions to cognitive impairment and dementia: a statement for healthcare professionals from the American heart association/American stroke association. *Stroke* 2011; 42: 2672–2713.
14. Rader DJ, Cohen J and Hobbs HH. Monogenic hypercholesterolemia: new insights in pathogenesis and treatment. *J Clin Invest* 2003; 111: 1795–1803.
15. Zadelaar S, Kleemann R, Verschuren L, et al. Mouse models for atherosclerosis and pharmaceutical modifiers. *Arterioscler Thromb Vasc Biol* 2007; 27: 1706–1721.
16. Mulder M, Jansen PJ, Janssen BJ, et al. Low-density lipoprotein receptor-knockout mice display impaired spatial memory associated with a decreased synaptic density in the hippocampus. *Neurobiol Dis* 2004; 16: 212–219.
17. de Oliveira J, Hort MA, Moreira EL, et al. Positive correlation between elevated plasma cholesterol levels and cognitive impairments in LDL receptor knockout mice: relevance of cortico-cerebral mitochondrial dysfunction and oxidative stress. *Neuroscience* 2011; 197: 99–106.
18. Zhao L, Ding T, Cyrus T, et al. Low-dose oral sirolimus reduces atherogenesis, vascular inflammation and modulates plaque composition in mice lacking the LDL receptor. *Br J Pharmacol* 2009; 156: 774–785.
19. Pakala R, Stabile E, Jang GJ, et al. Rapamycin attenuates atherosclerotic plaque progression in apolipoprotein E knockout mice: inhibitory effect on monocyte chemotaxis. *J Cardiovasc Pharmacol* 2005; 46: 481–486.
20. Lin AL, Zheng W, Halloran JJ, et al. Chronic rapamycin restores brain vascular integrity and function through NO synthase activation and improves memory in symptomatic mice modeling Alzheimer's disease. *J Cereb Blood Flow Metab* 2013; 33: 1412–1421.
21. Harrison DE, Strong R, Sharp ZD, et al. Rapamycin fed late in life extends lifespan in genetically heterogeneous mice. *Nature* 2009; 460: 392–395.
22. Johnson SC, Yanos ME, Bitto A, et al. Dose-dependent effects of mTOR inhibition on weight and mitochondrial disease in mice. *Front Genet* 2015; 6: 247.
23. Frick KM and Berger-Sweeney J. Spatial reference memory and neocortical neurochemistry vary with the estrous cycle in C57BL/6 mice. *Behav Neurosci* 2001; 115: 229–237.
24. Frye CA. Estrus-associated decrements in a water maze task are limited to acquisition. *Physiol Behav* 1995; 57: 5–14.
25. Elder GA, Ragnauth A, Dorr N, et al. Increased locomotor activity in mice lacking the low-density lipoprotein receptor. *Behav Brain Res* 2008; 191: 256–265.
26. Girotti M, Donegan JJ and Morilak DA. Chronic intermittent cold stress sensitizes neuro-immune reactivity in the rat brain. *Psychoneuroendocrinology* 2011; 36: 1164–1174.
27. Zamora DA, Downs KP, Ullevig SL, et al. Glutaredoxin 2a overexpression in macrophages promotes mitochondrial dysfunction but has little or no effect on atherogenesis in LDL-receptor null mice. *Atherosclerosis* 2015; 241: 69–78.
28. Qiao M, Kisgati M, Cholewa JM, et al. Increased expression of glutathione reductase in macrophages decreases atherosclerotic lesion formation in low-density lipoprotein receptor-deficient mice. *Arterioscler Thromb Vasc Biol* 2007; 27: 1375–1382.
29. Barman SA, Chen F, Su Y, et al. NADPH oxidase 4 is expressed in pulmonary artery adventitia and contributes

to hypertensive vascular remodeling. *Arterioscler Thromb Vasc Biol* 2014; 34: 1704–1715.
30. Morris R. Developments of a water-maze procedure for studying spatial learning in the rat. *J Neurosci Meth* 1984; 11: 47–60.
31. Duong TQ, Silva AC, Lee SP, et al. Functional MRI of calcium-dependent synaptic activity: cross correlation with CBF and BOLD measurements. *Magn Reson Med* 2000; 43: 383–392.
32. Jensen JH and Chandra R. MR imaging of microvasculature. *Magn Reson Med* 2000; 44: 224–230.
33. Zhang Y, Bokov A, Gelfond J, et al. Rapamycin extends life and health in C57BL/6 mice. *J Gerontol Ser A* 2014; 69: 119–130.
34. Spilman P, Podlutskaya N, Hart MJ, et al. Inhibition of mTOR by rapamycin abolishes cognitive deficits and reduces amyloid-beta levels in a mouse model of Alzheimer's disease. *PloS One* 2010; 5: e9979.
35. Halloran J, Hussong SA, Burbank R, et al. Chronic inhibition of mammalian target of rapamycin by rapamycin modulates cognitive and non-cognitive components of behavior throughout lifespan in mice. *Neuroscience* 2012; 223: 102–113.
36. Baar EL, Carbajal KA, Ong IM, et al. Sex- and tissue-specific changes in mTOR signaling with age in C57BL/6J mice. *Aging Cell* 2016; 15: 155–166.
37. Tardif S, Ross C, Bergman P, et al. Testing efficacy of administration of the antiaging drug rapamycin in a non-human primate, the common marmoset. *J Gerontol Ser A* 2015; 70: 577–587.
38. Fok WC, Chen Y, Bokov A, et al. Mice fed rapamycin have an increase in lifespan associated with major changes in the liver transcriptome. *PloS One* 2014; 9: e83988.
39. d Oliveira RB, Carvalho CP, Polo CC, et al. Impaired compensatory beta-cell function and growth in response to high-fat diet in LDL receptor knockout mice. *Int J Exp Pathol* 2014; 95: 296–308.
40. Houde VP, Brule S, Festuccia WT, et al. Chronic rapamycin treatment causes glucose intolerance and hyperlipidemia by upregulating hepatic gluconeogenesis and impairing lipid deposition in adipose tissue. *Diabetes* 2010; 59: 1338–1348.
41. Brown NF, Stefanovic-Racic M, Sipula IJ, et al. The mammalian target of rapamycin regulates lipid metabolism in primary cultures of rat hepatocytes. *Metabolism* 2007; 56: 1500–1507.
42. Sivendran S, Agarwal N, Gartrell B, et al. Metabolic complications with the use of mTOR inhibitors for cancer therapy. *Cancer Treat Rev* 2014; 40: 190–196.
43. Kurdi A, De Meyer GR and Martinet W. Potential therapeutic effects of mTOR inhibition in atherosclerosis. *Br J Clin Pharmacol* 2015; 82: 1267–1279.
44. Martin AJ, Friston KJ, Colebatch JG, et al. Decreases in regional cerebral blood flow with normal aging. *J Cereb Blood Flow Metab* 1991; 11: 684–689.
45. Noda A, Ohba H, Kakiuchi T, et al. Age-related changes in cerebral blood flow and glucose metabolism in conscious rhesus monkeys. *Brain Res* 2002; 936: 76–81.
46. Williams KJ and Tabas I. The response-to-retention hypothesis of early atherogenesis. *Arterioscle Thromb Vasc Biol* 1995; 15: 551–561.
47. Sadowski M, Pankiewicz J, Scholtzova H, et al. Links between the pathology of Alzheimer's disease and vascular dementia. *Neurochem Res* 2004; 29: 1257–1266.
48. Fischer KE, Gelfond JA, Soto VY, et al. Health effects of long-term rapamycin treatment: the impact on mouse health of enteric rapamycin treatment from four months of age throughout life. *PloS One* 2015; 10: e0126644.
49. Holdaas H, Potena L and Saliba F. mTOR inhibitors and dyslipidemia in transplant recipients: a cause for concern? *Transplant Rev* 2014; 29: 93–102.
50. Morrisett JD, Abdel-Fattah G, Hoogeveen R, et al. Effects of sirolimus on plasma lipids, lipoprotein levels, and fatty acid metabolism in renal transplant patients. *J Lipid Res* 2002; 43: 1170–1180.
51. Mueller MA, Beutner F, Teupser D, et al. Prevention of atherosclerosis by the mTOR inhibitor everolimus in LDLR-/- mice despite severe hypercholesterolemia. *Atherosclerosis* 2008; 198: 39–48.
52. Ishibashi S, Brown MS, Goldstein JL, et al. Hypercholesterolemia in low density lipoprotein receptor knockout mice and its reversal by adenovirus-mediated gene delivery. *J Clin Invest* 1993; 92: 883–893.
53. Martinet W, De Loof H and De Meyer GR. mTOR inhibition: a promising strategy for stabilization of atherosclerotic plaques. *Atherosclerosis* 2014; 233: 601–607.
54. Wang X, Li L, Li M, et al. Knockdown of mTOR by lentivirusmediated RNA interference suppresses atherosclerosis and stabilizes plaques via a decrease of macrophages by autophagy in apolipoprotein Edeficient mice. *Int J Mol Med* 2013; 32: 1215–1221.
55. Peng N, Meng N, Wang S, et al. An activator of mTOR inhibits oxLDL-induced autophagy and apoptosis in vascular endothelial cells and restricts atherosclerosis in apolipoprotein E(-)/(-) mice. *Sci Rep* 2014; 4: 5519.
56. Waksman R, Pakala R, Burnett MS, et al. Oral rapamycin inhibits growth of atherosclerotic plaque in apoE knock-out mice. *Cardiovasc Radiat Med* 2003; 4: 34–38.
57. Chiao YA, Kolwicz SC, Basisty N, et al. Rapamycin transiently induces mitochondrial remodeling to reprogram energy metabolism in old hearts. *Aging* 2016; 8: 314–327.
58. Hebert M, Licursi M, Jensen B, et al. Single rapamycin administration induces prolonged downward shift in defended body weight in rats. *PloS One* 2014; 9: e93691.
59. Tenderich G, Fuchs U, Zittermann A, et al. Comparison of sirolimus and everolimus in their effects on blood lipid profiles and haematological parameters in heart transplant recipients. *Clin Transplant* 2007; 21: 536–543.
60. Fang Y, Westbrook R, Hill C, et al. Duration of rapamycin treatment has differential effects on metabolism in mice. *Cell Metab* 2013; 17: 456–462.
61. Polak P, Cybulski N, Feige JN, et al. Adipose-specific knockout of raptor results in lean mice with enhanced mitochondrial respiration. *Cell Metab* 2008; 8: 399–410.

62. Johnson SC, Yanos ME, Kayser EB, et al. mTOR inhibition alleviates mitochondrial disease in a mouse model of Leigh syndrome. *Science* 2013; 342: 1524–1528.
63. Luchsinger JA and Mayeux R. Cardiovascular risk factors and Alzheimer's disease. *Curr Atheroscler Rep* 2004; 6: 261–266.
64. de Bruijn RF and Ikram MA. Cardiovascular risk factors and future risk of Alzheimer's disease. *BMC Med* 2014; 12: 130.
65. Fillit H, Nash DT, Rundek T and Zuckerman A. Cardiovascular risk factors and dementia. *Am J Geriatr Pharmacother* 2008; 6: 100–118.
66. Franciosi S, Gama Sosa MA, English DF, et al. Novel cerebrovascular pathology in mice fed a high cholesterol diet. *Mol Neurodegener* 2009; 4: 42.
67. Sanan DA, Newland DL, Tao R, et al. Low density lipoprotein receptor-negative mice expressing human apolipoprotein B-100 develop complex atherosclerotic lesions on a chow diet: no accentuation by apolipoprotein(a). *Proc Natl Acad Sci U S A* 1998; 95: 4544–4549.
68. Wilkinson JE, Burmeister L, Brooks SV, et al. Rapamycin slows aging in mice. *Aging Cell* 2012; 11: 675–682.
69. Cleary C, Linde JA, Hiscock KM, et al. Antidepressive-like effects of rapamycin in animal models: implications for mTOR inhibition as a new target for treatment of affective disorders. *Brain Res Bull* 2008; 76: 469–473.
70. Galkina E and Ley K. Immune and inflammatory mechanisms of atherosclerosis (*). *Annu Rev Immunol* 2009; 27: 165–197.
71. Libby P, Ridker PM and Maseri A. Inflammation and atherosclerosis. *Circulation* 2002; 105: 1135–1143.
72. Weichhart T, Costantino G, Poglitsch M, et al. The TSC-mTOR signaling pathway regulates the innate inflammatory response. *Immunity* 2008; 29: 565–77.
73. Perl A. Activation of mTOR (mechanistic target of rapamycin) in rheumatic diseases. *Nat Rev Rheumatol* 2016; 12: 169–182.
74. Lee HY, Kim MK, Park KS, et al. Serum amyloid A stimulates matrix-metalloproteinase-9 upregulation via formyl peptide receptor like-1-mediated signaling in human monocytic cells. *Biochem Biophys Res Commun* 2005; 330: 989–998.